Journal of Materials Chemistry A

Accepted Manuscript

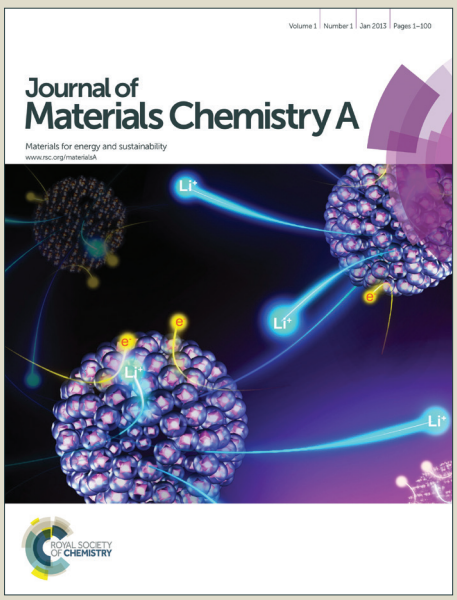

ROYAL SOCIETY OF CHEMISTRY

www.rsc.org/materialsA

Journal Name

RSCPublishing

ARTICLE

Hierarchically Structured WO_3-CNT@TiO_2NS composite with the Enhanced Photocatalytic Activity

Cite this: DOI: 10.1039/x0xx00000x

Shixiong Li [a], Zhefei Zhao [a], Yicao Huang [a], Jing Di [a,b], Yi (ALec) Jia [c] and Huajun Zheng* [a,b]

Received 00th January 2012,
Accepted 00th January 2012

DOI: 10.1039/x0xx00000x

www.rsc.org/

A novel hierarchically structured WO_3-CNTs@TiO_2NS composite was prepared by the combination of solvothermal and liquid-phase chemistry deposition technique. The obtained composite has highly rough and porous structure with WO_3 nanoparticles distributed uniformly on the surface. The photocatalytic performance was tested by photocatalytic degradation of methylene blue. It is indicate that the WO_3-CNT@TiO_2NS composite shows more remarkable improvement of the photocatalytic performance than that of the CNT@TiO_2NS. In particular, the presence of 15 wt% WO_3 reaches the highest photocatalytic activity, which is 4 times than that of CNT@TiO_2NS. The enhanced photocatalytic properties are mainly attributed to the more efficient photogenerated carrier separation, enhanced light absorption as well as the higher adsorption ability. It is suggested that WO_3 deposition is a promising way to enhance the photocatalytic activity of TiO_2-based photocatalyst.

1. Introduction

In the recent decade, semiconductors used as photocatalytic materials for the decomposition of organic pollutants have attracted many researchers' attention owing to their fundamental and technological applications to environmental purification[1, 2]. The pioneer of these materials is titanium dioxide (TiO_2) firstly reported by Fujishima[3]. TiO_2 , as many researchers proved, can break down a variety of organic pollutants under UV-light irradiation[4], which makes it an outstanding semiconductor photocatalyst. However, duo to the limited capability of absorbing visible and infrared light, as well as the rapid combination of photogenerated electrons and holes, there have been persistent efforts to improve the photocatalysis performance of TiO_2.

One promising strategy is to composite TiO_2 with other materials. Taking account of the poor conductivity of TiO_2, addition of conductive materials such as metals[5-8], polymers[9, 10] and carbon nanotubes[11-13] has been widely practiced. Compared with the conventional conductive additives, carbon nanotube (CNT) has synergistic effect with TiO_2, which can greatly lower the recombination rate of photogenerated electrons and holes[13-17]. B. Ráti et al[13] reported that CNT can not only act as conductive wires that can transfer and store photogenerated electrons thus increasing the lifetime of the separated charge carriers, but also play a role of absorbent improving the photocatalytic performance of the TiO_2/CNT composite samples. Besides, a number of works have showed that incorporation of WO_3 is also an efficient root to improve the photocatalytic activity under both UV and visible light with the enhanced light absorption and reduced electron–hole recombination. Zhan.et al[18] reported that the photocatalytic activity of TiO_2/WO_3 nanocomposite film is five times higher than that of pure TiO_2 film and eight times higher than that of pure WO_3 film duo to the formation of heterojunction between TiO_2 and WO_3 nanoparticles which can facilitate the separation of photo-generated electron–hole pairs. Flam-made[19] WO_3/TiO_2 particles exhibit improved photocatalytic activity because of the increased surface acidity and better charge separation. Xiao et al[20] have synthesized WO_3/TNTs nanocomposites which exhibit enhanced photocatalytic activity toward Rhodamine B degradation due to the reduction of electron-hole recombination and the enlargement of light absorption scope for photoexcitation. Up to now, although plenty of works have been devoted to fabricating CNT/TiO_2 and TiO_2/WO_3 composites, rare articles can be found with respect to the photocatalytic performance of the hierarchical isomeric composites containing TiO_2, WO_3 and CNT[21-23]. Furthermore, a comprehensive mechanism understanding of WO_3 in enhancing light absorption and retarding electron–hole pair recombination, especially improving overall adsorption performances of the catalysts, is also highly desired.

In the present paper, we demonstrate our strategy in designing the novel ternary complex composed of three basic

constitutional units, that is, TiO_2 nanosheet (NS), WO_3 nanoparticle and CNT. Our design starts from acid-treated CNT with some hydroxyl groups (OH^-) or carboxyl groups on its surfaces. The TiO_2 NS are epitaxially grown onto the CNT via a solvothermal synthesis technique, which provides ample 'active sites' for additional WO_3 nanoparticle germination onto the surface of the well-aligned TiO_2 NS. As narrow gap semiconductor WO_3 can absorb visible light, thus extending the photoexcitation energy range. Moreover, WO_3 has a higher affinity for chemical species, which is important for photocatalytic reaction[24-26]. Furthermore, the energy levels of WO_3 and TiO_2 is matched very well[21, 27, 28], electrons can be easily transferred from the conduction band of TiO_2 to WO_3, then improve the charge separation efficiency. To the best of our knowledge, it is the first time to synthesize and utilize the hierarchically structured WO_3-CNT@TiO_2NS composite for photodegradation of organic contaminants. Moreover, the photocatalytic properties of the as-prepared WO_3-CNT@TiO_2NS composite and the effect of WO_3 on the photocatalytic activity were systematically investigated.

2. Experimental section

2.1 Materials

Multi-walled carbon nanotube (CNT purity>95%) with a diameter of 40-60 nm and length of 5-15 μm, was purchased from Nanotech Port Co, Ltd. (Shenzhen, China). Dimethylformide (DMF), isopropyl alcohol (IPA) and nitric acid (HNO_3 65%) were supplied by Aldrich Chemical Company. Tetrabutyl titanate (TBT) and tungsten hexachloride (WCl_6 99%) were purchased from the Aladdin Industrial Corporation. All chemical reagents are analytical grade and were used without further purification.

2.2 Preparation of WO_3-CNT@TiO_2NS composite

Prior to TiO_2 coating, the pristine CNT were pretreated in concentrated nitric acid at 180 ℃ for 6 h to remove metal catalysts as well as to introduce carboxyl groups on the CNT surface. The acid-treated CNT was first dispersed in a clear solution containing 15 mL DMF and 45mL isopropyl alcohol (IPA) with sonication for 30 minutes, and then 2 mL of TBT was added into the obtained solution under gentle stirring, which was subsequently transferred into a 100 mL Teflon-lined stainless steel autoclave and kept in an electric oven at 200 ℃ for 10 h. The resulting precursor was washed with ethanol, dried at 60 ℃ overnight. To prepare WO_3-CNT@TiO_2NS, CNT@TiO_2NS composites was added into 25 mL of dehydrated alcohol solution dissolved with different stoichiometric amount of WCl_6. Then the suspension was stirring at room temperature for 2 h and dried at 60 ℃, followed by a calcination treatment at 450 ℃ in air for 2 h. For comparison, pure CNT@TiO_2NS and different WO_3 content of WO_3-CNT@TiO_2NSs were also prepared using the similar procedures.

2.3 Materials Characterization

The product morphology and microstructure was observed on a scanning electron microscope (SEM, Hitachi S-4800). A transmission electron microscopy (TEM, JEOL, JEM200CX, JEOL) with Energy dispersive X-ray spectroscopy (EDS, BRUKER AXS) was carried out to analyze the chemical compositions and structural information of the samples. Powder X-ray diffraction (XRD, Bruker D8 Advance diffractometer with Cu-Kα radiation) experiments were performed to study the crystallographic information of the samples. The UV–vis spectra of the solid samples were taken by Cary 5000 UV–Vis-NIR spectrophotometer equipped with an integrating sphere.

2.4 Photocatalytic test

The liquid phase photodegradation of methylene blue (MB) activity test was carried out in a self-designed 150 mL reactor at room temperature under air. Before photocatalytic reaction, 0.05 g samples were dispersed in 100 mL MB (15 mg/L) aqueous solution and magnetically stirred for 30 min in the dark to achieve the adsorption equilibrium. The photocatalysis was started by irradiating the reaction mixture with a 300 W xenon lamp and stirred at the speed of 400 rpm to eliminate the diffusion effects. At regular irradiation time intervals, aliquots (4 mL) were sampled and centrifuged to separate the suspended catalysts. The residual MB concentration was detected by Shimadzu UV-1800 spectrophotometer at its characteristic wavelength (λ= 664 nm), from which the degradation yield could be calculated.

3. Results and discussion

3.1 XRD analysis

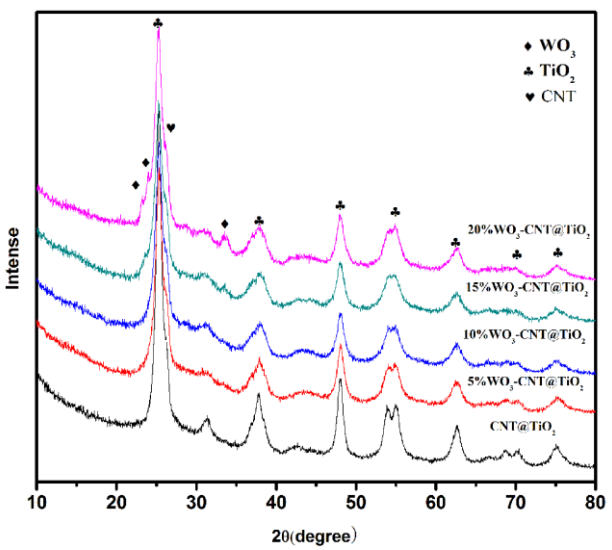

Fig 1 XRD patterns of the as-prepared CNT@TiO_2NS and WO_3–CNT@TiO_2NS composite

Journal Name

RSCPublishing

ARTICLE

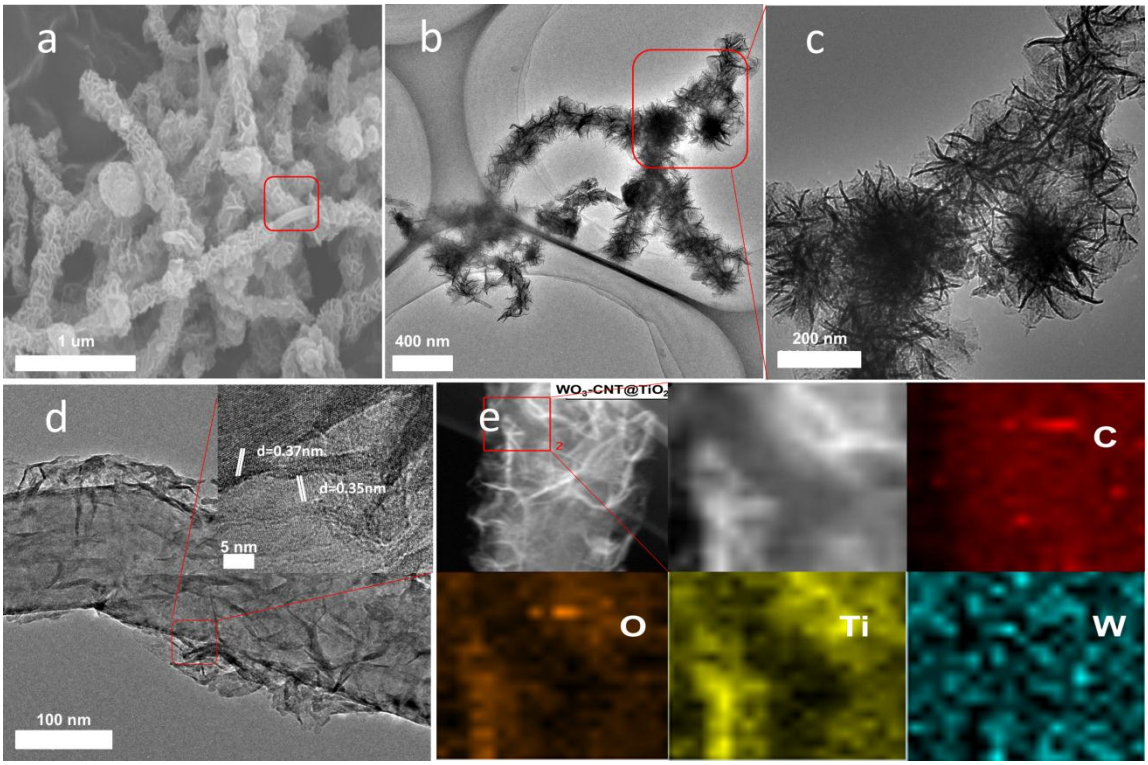

Fig 2 Characterization results of the as-prepared 15%WO_3–CNT@TiO_2NS nanocomposite: SEM image (a); TEM image (b, c and d); elemental mapping image (e).

The XRD results of the CNT@TiO_2 and WO_3–CNT@TiO_2NS composite are shown in Fig 1. In the XRD patterns of the CNT@TiO_2 composite, the diffraction peaks at 25.3°, 37.9°, 48.0°, 54.0°, 55.0°, and 62.5° assigned to diffraction planes of (101), (004), (200), (105), (211), and (204) of anatase (JCPDS 071-1166) is sharp because of the high TiO_2 content and high crystallinity. The peak at about 26.3° corresponding to (002) plane of CNT (JCPDS 008-0415) almost overlaps with the (101) peak of anatase TiO_2, making it difficult to discern from the current diffraction pattern. For the WO_3–CNT@TiO_2NS composites, the diffraction peaks of orthorhombic WO_3 (JCPDS 020-1324) crystallites at 23.1°, 24.0° and 33.5° is very weak and the relative intensity of crystal planes increased slightly with the increase of WO_3 content in the composite. It is indicate that the two type particles are dispersed uniformly in the composite and the coupling of WO_3 particles has little influence on the crystal phase of TiO_2 particles but the relative intensity of crystal planes.

3.2 Morphologies and structures

The surface morphology and microstructure of the synthesized samples were characterized by scanning electron microscopy (SEM) and transmission electronmicroscopy (TEM). Fig 2a shows a panoramic view of the as-prepared WO_3–CNT@TiO_2 NS nanocomposite by SEM. The composite displays sinuous and highly entangled one-dimensional structure with a rough and porous surface morphology. The diameter observed from the image is about 200 nm. The specially selected red rectangle frame part of SEM image and the TEM image in Fig 2b reveals a hierarchically structured surface morphology as characterized by assembly of nanosheet-like structures onto CNT backbones, forming parasitic architecture. Unquestionably, the hierarchical porous structures provide considerable specific surface area to ensure fully utilization of the photoactive materials and also offer numerous material channels to improve the photocatalytic performances. From the magnified TEM image of WO_3–CNT@TiO_2NS composite in Fig 2c and d, it can be seen that CNTs in the composite are uniformly encapsulated by TiO_2 ultrathin NS structures along with the longitudinal axis. At the same time, WO_3 nanoparticles appear as the black spots which are distributed uniformly on the surface of CNT@TiO_2. This is further verified by elemental mapping images which demonstrate the distributions of all the elements. Furthermore, High-resolution TEM (HRTEM) image shown in Fig 2d reveals that the composite has distinct lattice fringes with an interplanar spacing of 0.35 nm, corresponding well to the (101) plane of

anatase and another interplanar spacing of 0.37 nm corresponding well to the (200) plane of WO_3.

3.3 UV-Vis spectra

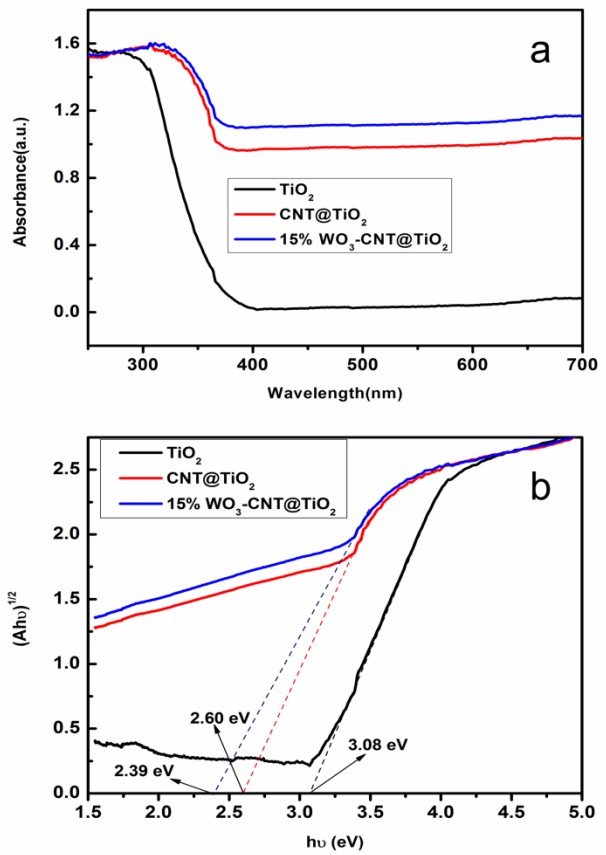

Fig 3 (a) UV-Vis absorption spectra of pure TiO_2, CNT@TiO_2NS and 15%WO_3–CNT@TiO_2NS and (b) The derived plots of transformed Kubelka-Munk function for these three samples versus the energy of light.

The UV-Vis absorption spectra of the pure TiO_2, CNT@TiO_2NS and 15%WO_3–CNT@TiO_2NS composite are shown in Fig 3a. It can be seen that both of the CNT@TiO_2NS and 15%WO_3–CNT@TiO_2NS catalysts exhibit a stronger visible light absorption than the pure TiO_2. Besides, the absorption edge of them also shifted towards the longer wavelength side, which indicates an ability of the composites to be photoactivated under the visible light irradiation. On the one hand, this may be ascribed to the porous surface structure of the CNT@TiO_2NS and 15%WO_3–CNT@TiO_2NS composite, which is believed to favor the harvesting of light owe to maximized reflections and scatter efficiency within the porous framework. On the other hand, the deposition of CNT is good for the light-absorbing properties of the composites for its broad light absorption ability. Moreover, in the visible light region, a further increase in the absorption intensity of 15%WO_3–CNT@TiO_2NS samples is observed. This phenomenon should be ascribed to the deposition of WO_3, which has strong visible light absorption for its intrinsic narrow band gap. Fig. 3b plots the relationship of modified Kubelka-Munk function, $(Ah\upsilon)^{1/2}$, versus photon energy. The result indicates that the bandgap (Eg) of TiO_2 was 3.08 eV, which was similar to the reported Eg value of TiO2. Meanwhile, the observed bandgap value for 15%WO_3–CNT@TiO_2NS was 2.39 eV, shown a slight red-shift to the CNT@TiO_2NS (2.60 eV). Therefore, modification with WO_3 can not only increase visible-light absorption but also provides a red shift in absorption to higher wavelengths. This result is corresponding well to the previously reported WO_3-TiO_2 materials.

3.4 Photoelectrical response properties

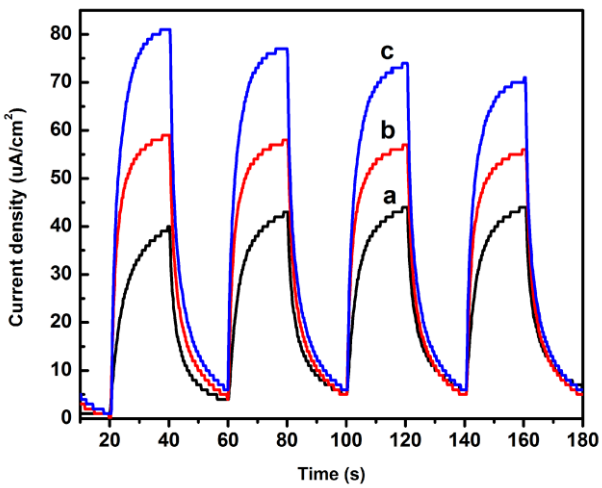

Fig 4 Photocurrent responses of (a) pure TiO_2, (b) CNT@TiO_2NS and (c) 15%WO_3–CNT@TiO_2NS composite under the whole wavelength light irradiation.

In order to prove the point that enhancement of light absorption can improve the photocatalytic activity in electrochemical terms and understand the electron transfer in the WO_3–CNT@TiO_2NS composites, transient photocurrent experiments were performed under discontinuous illumination. The results are shown in Fig. 4. It demonstrated that the composition of the composite influences obviously the photocurrent density of the electrode and an increase order of TiO_2<CNT@TiO_2<15%WO_3–CNT@TiO_2NS in terms of photocurrent are observed. This result matches well with the data of light absorption order. The maximum photocurrent density for the 15%WO_3–CNT@TiO_2NS electrode is 80 uA•cm^{-2}, which is 1.4 and 2 times as high as that of the CNT@TiO_2 and TiO_2 electrode respectively. This phenomenon suggesting that WO_3 has an positive synergetic effect with CNT@TiO_2NS, which can not only enhance light absorption but also facilitate the separation of photoinduced electrons and holes.

Journal Name

RSCPublishing

ARTICLE

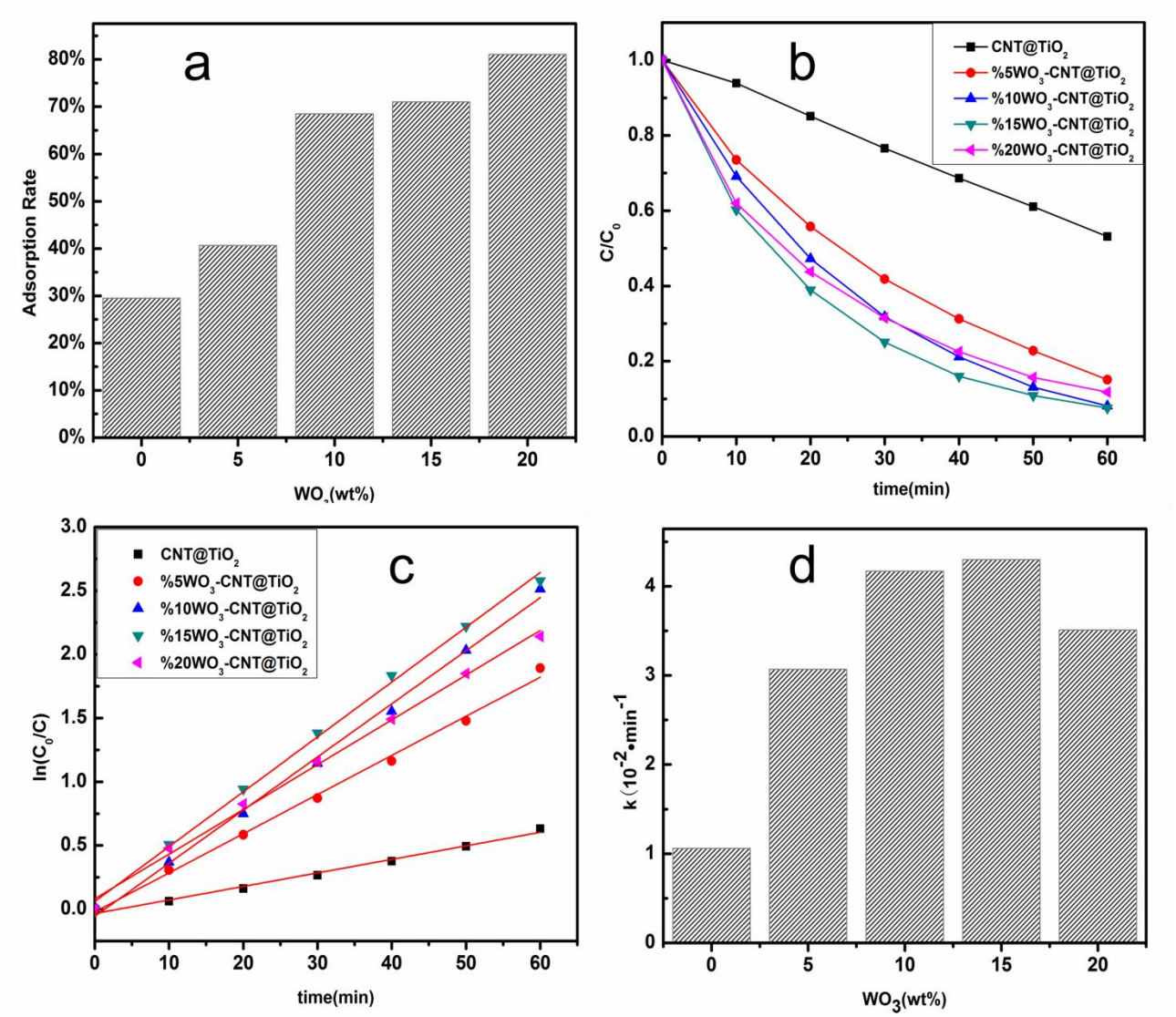

Fig 5 Photocatalytic degradation of MB using different samples as catalysts: (a) the adsorption abilities (b) photodegradation (c) reaction kinetic curves (d) the reaction rate constant (k) values comparison.

3.5 Catalytic Properties

Photocatalytic reactions, as everyone knows, are very complex. Among all these factors, the properties of light absorption and catalysts adsorption, as well as the efficiency of photon-generated carrier separation are the most important ones. The photocatalytic activity of the samples was evaluated by measuring the rate of degradation of MB solution with photocatalyst.

Adsorption, as a prerequisite for good photocatalytic activity, is an important factor to enhance the photoactivity. In this study, MB solution (15 mg/L) was used as the example pollutant to assess the adsorption performances of the photocatalysts. The suspension solution containing 100 mL of MB and 0.05 g photocatalyst composites was stirred in the dark for 30 min to establish adsorption-desorption equilibrium. From the Fig 5a, it can be seen that with WO_3 content increasing adsorption rates of the WO_3–CNT@TiO_2NS composites increased significantly. As previous reported, WO_3 is about 15

times more acidic than TiO_2[25]. Hence, we believe that it is mainly because of the increase in surface acidity with WO_3 concentration increasing. The photodegradation rate of different photocatalysts was tested with the photocatalytic degradation of MB solution. In Fig 5b, it is clearly observed that the WO_3–CNT@TiO_2 NS composite exhibits much higher photocatalytic activity than that of CNT@TiO_2 NS photocatalysts, 92.4% of MB is degraded by 15%WO_3–CNT@TiO_2 NS within 1 h irradiation. However, the photocatalytic activity of pure CNT@TiO_2NS is much lower, only 46.9% of MB is degraded. In order to Investigate the degradation kinetics and quantitatively compare of the photocatalytic property of these samples, the pseudo first order kinetics equation ($\ln(C_0/C)=kt$) was adopted to describe the experimental data. In the above equation, k reflects the reaction rate constant and its values is derived from the slopes of the linear curves of $\ln(C_0/C)$ versus irradiation time (t) for MB degradation in Fig 4c. The k value is shown in Fig 5d. By the incorporation of WO_3 into the CNT@TiO_2NS composite, the photocatalytic activity was enhanced. The photocatalytic activity was maximized at 15%wt of WO_3 coated and the photocatalytic degradation rate constant for the 15%WO_3–CNT@TiO_2NS is 4.3×10^{-2}•min^{-1}, which is about 4 times higher than that of CNT@TiO_2NS.

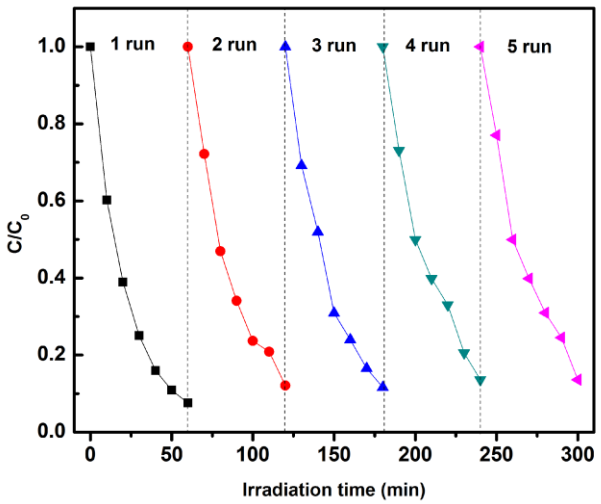

Fig 6 Cyclic photodegradation of MB by 15%WO_3-CNT@TiO_2NS composite

To evaluate the stability of 15%WO_3-CNTs@TiO_2NS composite, the recyclability of the catalyst for photodegradation of MB was conducted. The result is shown in Fig 6. After 5 times photocatalytic cyclic reaction, the photocatalytic activity of 15% WO_3-CNTs@TiO_2NS composite only decreases a little, suggesting the good stability of the photocatalyst.

According to the above experimental research analysis and the previous work[25, 26, 29], we hold the opinion that the significant enhance of photocatalytic ability is mainly caused by the deposited WO_3. With the introduction of WO_3, the surface acidity and affinity of the WO_3–CNT@TiO_2 NS composite is increased due to the highly acidic nature of WO_3. Hence the photocatalysts can adsorb a greater amount of OH^- or H_2O, which is important for the generation of •OH radicals[19, 25, 30]. At the same time, MB molecules can be easily adsorbed on its surface, which are necessary to initiate the photocatalytic reaction. Moreover, the WO_3–CNT@TiO_2NS composite exhibits an obvious red shift in the absorption wavelength range and has higher absorption intensity in the visible region, thus more charge carriers are generated to take part in the photocatalytic reaction. Besides, the energy band structure of the TiO_2 and WO_3 is matched very well[21, 27, 28]. The photoelectrons can easily migrate from the TiO_2 surfaces to the WO_3 conduction band and was captured by the surface adsorbed O_2. Then the yielded superoxide anions attack the MB molecules directly or generate hydroxyl radicals to degrade MB. At the meantime, photogenerated holes transfer could take place from the valence band (VB) of WO_3 to the VB of TiO_2, then captured by hydroxyl groups(OH^-) or H_2O on the photocatalyst surface and yielded hydroxyl radicals or scavenged by the MB[21, 23]. This resulted in a decrease in the electron−hole pair recombination. Therefore, all of these advantageous factors lead to the high photocatalytic activity of our products.

4. Conclusions

We present the design, preparation and testing of WO_3–CNT@TiO_2NS composite for photocatalytic degradation of methylene blue (MB). Compared to the CNT@TiO_2NS composite, the sample of WO_3–CNT@TiO_2NS composite exhibits much higher catalytic activity, especially 15%WO_3–CNT@TiO_2NS composite, its rate constant of degradation is 4 times of that of CNT@TiO_2NS. It is believed that the enhanced photocatalytic activity originates from the more efficient photogenerated carriers separation, light absorption as well as the significantly enhanced chemical species adsorbability, whereas the introduction of appropriate amount of WO_3 contributes much to the above-mentioned performance for its synergistic effect with CNT@TiO_2NS. The result of the present work implies that choosing proper material with complementary advantages and cooperation potentials to form hybrid photocatalyst with reasonable structure design is a promising method to prepare high-activity catalyst.

Acknowledgements

The financial support from Zhejiang scientific and technological projects (NO. 2009R50002-20) is gratefully acknowledged.

Notes and references

[a] Department of Applied chemistry, Zhejiang University of Technology, Hangzhou 310014, China. E-mail: zhenghj@zjut.edu.cn.
[b] State Key Laboratory Breeding Base of Green Chemistry Synthesis Technology, Zhejiang University of Technology, Hangzhou 310014, PR China.
[c] Queensland Micro- and Nanotechnology Centre (QMNC), Griffith University, Nathan, QLD 4111

1. M. Kitano, M. Matsuoka, M. Ueshima and M. Anpo, *Applied Catalysis A: General*, 2007, **325**, 1-14.
2. X. Chen and S. S. Mao, *Chem. Rev*, 2007, **107**, 2891-2959.
3. F. A and H. K, *Nature*, 1972, **37**.
4. D. Y. Goswami, *J Sol Energ-T Asme*, 1997, **119**, 101-107.
5. C. K. Ngaw, Q. Xu, T. T. Y. Tan, P. Hu, S. Cao and J. S. C. Loo, *Chemical Engineering Journal*, 2014, **257**, 112-121.
6. H. Liu, T. Liu, X. Dong and Z. Zhu, *Materials Letters*, 2014, **134**, 240-243.
7. C. Hsu, Y. Shen, Z. Wei, D. Liu and F. Liu, *Journal of Alloys and Compounds*, 2014, **613**, 117-121.
8. P. Hájková, J. Matoušek and P. Antoš, *Applied Catalysis B: Environmental*, 2014, **160-161**, 51-56.
9. K. Yang, K. Huang, Z. He, X. Chen, X. Fu and W. Dai, *Applied Catalysis B: Environmental*, 2014, **158-159**, 250-257.
10. F. J. Feliciano and O. C. Monteiro, *Journal of Materials Science & Technology*, 2014, **30**, 449-454.
11. H. Zhou, L. Liu, X. Wang, F. Liang, S. Bao, D. Lv, Y. Tang and D. Jia, *Journal of Materials Chemistry A*, 2013, **1**, 8525.
12. J. Yu, T. Ma and S. Liu, *Physical chemistry chemical physics : PCCP*, 2011, **13**, 3491-3501.
13. B. Réti, K. Mogyorósi, A. Dombi and K. Hernádi, *Applied Catalysis A: General*, 2014, **469**, 153-158.
14. C. Zhao, H. Luo, F. Chen, P. Zhang, L. Yi and K. You, *Energy & Environmental Science*, 2014, **7**, 1700.
15. S. Wang and S. Zhou, *Journal of hazardous materials*, 2011, **185**, 77-85.
16. M. M. Gui, S.-P. Chai, B.-Q. Xu and A. R. Mohamed, *Solar Energy Materials and Solar Cells*, 2014, **122**, 183-189.
17. M.-L. Chen, F.-J. Zhang and W.-C. Oh, *Journal of the Korean Ceramic Society*, 2010, **47**, 269-275.
18. W. T. Zhan, H. W. Ni, R. S. Chen, Z. Y. Wang, Y. W. Li and J. H. Li, *Thin Solid Films*, 2013, **548**, 299-305.
19. K. K. Akurati, A. Vital, J.-P. Dellemann, K. Michalow, T. Graule, D. Ferri and A. Baiker, *Applied Catalysis B: Environmental*, 2008, **79**, 53-62.
20. M. Xiao, L. Wang, X. Huang, Y. Wu and Z. Dang, *Journal of Alloys and Compounds*, 2009, **470**, 486-491.
21. L. Zhu, Z. Meng and W.-C. Oh, *Chinese Journal of Catalysis*, 2011, **32**, 926-932.
22. Z. Pap, É. Karácsonyi, L. Baia, L. C. Pop, V. Danciu, K. Hernádi, K. Mogyorósi and A. Dombi, *physica status solidi (b)*, 2012, **249**, 2592-2595.
23. l. zhu, z. d. meng, k. y. cho, t. ghosh and w. c. oh, *ASIAN JOURNAL OF CHEMISTRY*, 2013, **25**, 713-718.
24. F. Wang, C. Li and J. C. Yu, *Separation and Purification Technology*, 2012, **91**, 103-107.
25. Y. Tae Kwon, K. Yong Song, W. In Lee, G. Jin Choi and Y. Rag Do, *Journal of Catalysis*, 2000, **191**, 192-199.
26. B. Liu, J. Wang, J. Wu, H. Li, Z. Li, M. Zhou and T. Zuo, *Journal of Materials Chemistry A*, 2014, **2**, 1947.
27. W. Smith, A. Wolcott, R. C. Fitzmorris, J. Z. Zhang and Y. Zhao, *Journal of Materials Chemistry* 2011, **21**, 10792-10800.
28. Z.-F. Huang, J.-J. Zou, L. Pan, S. Wang, X. Zhang and L. Wang, *Applied Catalysis B: Environmental*, 2014, **147**, 167-174.
29. V. Puddu, R. Mokaya and G. Li Puma, *Chemical communications*, 2007, 4749-4751.
30. C. Y. Kuo, *Journal of hazardous materials*, 2009, **163**, 239-244.